Metabolomic Profiling of Brain Protective Effect of Edaravine on Cerebral Ischemia-reperfusion Injury in Mice

Hui-fen Ma
China Pharmaceutical University
Lin-jie Su
China Pharmaceutical University
Da-wei Zhang
China Pharmaceutical University
Shuai-shuai Gong
China Pharmaceutical University
Yi-ning Liu
China Pharmaceutical University
Yuan-yuan Zhang
China Pharmaceutical University
Fang Li
China Pharmaceutical University
Junping Kou (junpingkou@cpu.edu.cn)
China Pharmaceutical University https://orcid.org/0000-0001-8377-915X

Research

Keywords: Metabolomic, Edaravine, Ischemia stroke, Taurine, Endothelial cells

Posted Date: February 19th, 2021

DOI: https://doi.org/10.21203/rs.3.rs-214403/v1

Abstract

Edaravine (EDA) injection has seen extensively applied in clinic for treating stroke. Nevertheless, the metabolite signatures and underlying mechanisms associated with EDA remains unclear, which deserves further elucidation for improving the accuracy of EDA usage. Ischemia stroke was simulated by intraluminal occlusion of the right middle cerebral artery for 1 h followed by reperfusion for 24 h in mice. Brain infarct size, neurogical deficits and lactate dehydrogenase (LDH) level were improved by EDA. Significantly differential metabolites were screened with untargeted metabolomics by cross-comparisons with pre- and post-treatment of EDA under cerebral ischemia/reperfusion (I/R) injury. The possibly involved pathways, such as valine, leucine and isoleucine biosynthesis, phenylalanine metabolism, taurine and hypotaurine metabolism, were enriched with differential metabolites and relatively regulatory enzymes, respectively. The network of differential metabolites was constructed for integral exhibition of metabolic characteristics. Targeted analysis of taurine, an important metabolic marker, was performed for further validating. The decreased level of taurine was confirmed in MCAO/R mice and increased by EDA. The inhibition of EDA on cerebral endothelial cell apoptosis was confirmed by TdT-mediated dUTP nick-end labeling (TUNEL) stain. Cysteine sulfinic acid decarboxylase (CSAD), the rate-limiting enzyme of taurine generation, significantly increased along with inhibiting endothelial cells apoptosis after treatment of EDA. Thus, CSAD, as the possible new therapeutic target of EDA was selected and validated by western blotting and immunofluorescence. Together, this study provided the metabolite signatures and identified CSAD as an unrecognized therapeutic intervention for EDA in treatment of ischaemic stroke via inhibiting brain endothelial cells apoptosis.

Introduction

Stroke, one of the neurovascular diseases, is the leading cause of disability and death globally resulting from an increasing burden of vascular risk factors. Ischemic stroke is the most common type, accounting for 70% of all strokes [1, 2]. Although the precise mechanism underlying ischemic neuronal injury has not been fully elucidated, vascular pathology has been reported the most common cause. As a part of the vascular pathologies, endothelial cell (EC) death could affect the surrounding cellular environment, which made it a potential target mechanism for the treatment and prevention of stroke. And ECs line the entire microvasculature and are also important for maintaining normal brain function. Therefore, it is necessary to choose the appropriate drugs.

Edaravine injection (EDA), as a commonly neurovascular protective agent, has been widely used in patients with acute ischemic stroke owing to its scavenging effect on oxygen free radical and neurovascular protective effects [3]. It has been proved that EDA attenuates the Ca^{2+}-induced swelling of mitochondria and inhibits neurons apoptosis by decreasing the expression of Fas-associated death domain protein, death-associated protein, and caspase-8 immunoreactivity in the middle cerebral artery occlusion (MCAO) model [4]. EDA could suppress the response to endoplasmic reticulum stress and subsequent apoptotic signaling in hypoxic/ischemic injury and exhibit neuroprotective effects via its antioxidant actions, such as suppression of lipid peroxidation and oxidant-induced DNA damage [5, 6]. In

addition, EDA also could inhibit vascular endothelial growth factor expression, aquaporin-4 expression, nuclear factor-κB (NF-κB), inducible nitric oxide synthase (iNOS), cytokines, cyclooxygenase-2, reactive oxygen species (ROS) generation and ROS-induced inflammatory reactions in stroke mice and patients [3]. However, few of the literature comprehensively elucidates action characteristics of EDA, thus further studies are still needed.

Metabolites are small molecules (typically < 1.5 kDa) including lipids, amino acids, carbohydrates and nucleotides, that could reflect the downstream function of gene, protein expression and environmental changes, such as drugs intake, as a result, metabolome could provide information about related mechanisms [7]. What's more, disease-specific metabolites can be biomarkers for diagnosis of diseases and provide reference for precise use of drugs in clinic. The function characteristics of Huang-lian-jie-du decoction and gross saponins of *Tribulus terrestris* fruit were elucidated for ischemic stroke with matebolomics [8, 9]. By contrast, the value of metabolites of EDA for stroke has not been systematically studied. Therefore, the matebolomics were selected in order to investigate potential mechanism of EDA.

Herein, we intended to discover the therapeutic mechanism of EDA for stroke as comprehensively as possible according to the metabolite variation characteristics. In this study, untargeted metabolic profiling was applied to examined the serum and urine metabolic signature of EDA improvement of stroke. The metabolic network was constructed with differential metabolites. Finally, we performed targeted metabolic profiling and verified the potential therapeutic targets.

Materials And Methods

Chemicals and reagents

The standard compounds of taurine and caffeic acid were obtained from Shanghai yuanye Bio-technology Co.,Ltd (Shanghai, China). Deionized water used in experiment was supplied by a Milli-Q Academic ultra-pure water system (Milford, Millipore, USA). Acetonitrile and methanol were obtained from Merck (Chromatographic, Germany); formic acid was obtained from Tedia (Chromatographic, USA). Edaravone injection was from China national medicines Guorui pharmaceucital Co., Ltd (Anhui, China; lot number:2005018). Lactate dehydrogenase (LDH) assay kit was purchased from Nanjing Jiancheng Bioengineering Institute (Nanjing, China) and cysteine sulfinic acid decarboxylase (CSAD) was obtained from Abcam (Cambridge, England).

Animals and middle cerebral artery occlusion/reperfusion (MCAO/R) model

Adult male specified-pathogen-free (SPF) C57BL/6J mice weighing 18 - 22 g were obtained from the Experimental Animal Research Centre of Yangzhou University (Yangzhou, China; certificate no SCXK 2017 - 0007). All experimental protocols were performed according to the National Institutes of Health (NIH) guidelines and the research was approved by the Institutional Animal Care and Use Committee of the Animal Ethics Committee of the School of Chinese Materia Medica, China Pharmaceutical University. All mice were housed with a 12:12 h light-dark cycle at 23±1℃. Prior to experiments, mice were split

randomly into three groups: sham, MCAO/R and MCAOR+EDA. Stroke was induced by MCAO/R model in mice as reported previously [10]. Briefly, the right middle cerebral artery was occluded with a blunt-tip 6-0 nylon monofilament for 1 h followed with reperfusion for 24 h. Longa's method was used for evaluating neurological deficit [10]. Sham operated control mice underwent the same surgical procedures except for the occlusion by nylon monofilament. EDA was administrated intraperitoneally to mice with 3 mg/kg (refer to the clinical dose) after 1 h of ischemia, the remaining model mice were given an equal volume of normal saline.

Haematoxylin and Eosin (H&E) Staining

H&E staining was used for histomorphological analysis. In short, brain slices were put into haematoxylin and eosin solution, redehydrated in gradient ethanol solution again, treated with dimethylbenzene and covered with coverslips. The pathological images were scanned with a digital pathological section scanner (Hamamatsu, Japan) and analyzed with NDPView2 software.

TTC staining

After I/R, mice were euthanized and perfused by normal saline. Then, the whole brains were taken out, freezed at -20 degrees followed by cut into 1mm thick slices rapidly. These brain slices were incubated in 1 % TTC for 10 min at 37 °C. The infarcted areas were analyzed with Image J software (NIH, Bethesda, MD).

Transmission electron microscopy

After I/R, mice were euthanized and perfused by normal saline followed by perfusion with the fixative (2% glutaraldehyde and 2% lanthanum nitratein in 0.1M sodium cacodylate pH 7.4 - 7.5) at room temperature, as previously described [11]. 1 mm^3 sample obtained from the region encompassing ischemic infarction of removed brains were kept in the same fixative overnight at 4℃. The samples were post-fixed in 1% osmium tetroxide for 1h followed with embedded in Epon 812. After polymerization, three blocks were randomly selected from each brain sample. An Ultratome (Nova, LKB, Bromma, Sweden) was used for cutting ultrathin sections. Then, ultrath insections were mounted on mesh grids (6-8 sections/grid) and stained with uranyl acetate and lead citrate. Finally, the prepared samples were examined under a transmission electron microscope (JEOLLtd., Tokyo, Japan).

Untargeted metabolomics analysis

Sample pretreatment

Serum and urine of mice were collected after 24 hours reperfusion. After standing for about 60 minutes, the blood was centrifuged with 3500 r/min for 10 min at 15 °C. The obtained serum samples were sub-packed and stored in -80°C until the analysis. Urine samples were collected at 4 °C and kept at −80 °C until the analysis. 200 μL of serum and urine were used for untargeted metabolomics analysis and 600 μL of methanol was added into samples for precipitating protein. Samples were subsequently centrifuged

(13,000 rpm, 15 min) at 4 °C followed by swirling 60 s. The supernatant was transferred to a tube and dried under a gentle stream of nitrogen at room temperature. Then, the residue was dissolved with 200 μL methanol and centrifuged (13,000 rpm, 15 min) at 4 °C for further analysis.

HPLC-Q-TOF/MS analysis

The detection of metabolites in urine and serum samples was performed on an Agilent Technologies 6540 Accurate-Mass Q-TOF LC/MS (USA) with an electrospray ionization (ESI) source and the data were collected by mass hunter workstation. The eluent A and B were deionized water (0.1 % formic acid) and acetonitrile (0.1 % formic acid), respectively. Serum analyses were achieved on a SynergiTM Fusion-RP C18 column (50×2 mm i.d., 2.5 μm) with a gradient elution program: 0 - 5 min, 5 - 5% B; 5 - 10 min, 5 - 30% B; 10 - 15 min, 30 - 60% B; 15 - 20 min, 60 - 70% B; 20 - 22 min, 70 - 80% B; 22 - 25 min, 80 - 95% B; 25 - 30 min, 95 - 95% B. Urine analyses were achieved on a TSK-GEL Amide-80 column (150 × 2.0 mm i.d., 5 μm) with a gradient elution program: 0 - 7 min, 90 - 90% B; 7 - 9 min, 90 - 75% B; 9 - 11 min, 75 - 75% B; 11 - 13 min, 75 - 50% B;13 - 20 min, 50 - 50% B. Both of the flow rates were set at 0.2 mL/min with the injection volume of 10 μL. The Q-TOF/MS operating parameters were set as follows: fragment voltage, 120 V; nebulizer gas, 35 psig; capillary voltage, 4000 V; drying gas flow rate, 9 L/min; temperature, 325℃; detection range, m/z 50 - 1500 in full scan mass spectra. The MS data acquisition was carried out in positive and negative ionization mode.

Validation of system stability

Repeatability and robustness of the experiment were validated with the pooled quality control sample (QC) [12]. The QC sample was prepared to mix equal volumes (30 μL) of each test sample, and treated with the same method as the test samples. QC sample was randomly injected throughout the sequence list.

Data analysis of metabolomics strategies

Before multivariate analysis, the data format (.mzdata) files obtained by MassHunter Workstation Software (Version B.06.00, Agilent Technologies) were processed by XCMS software performing on the R+ package (R Foun-dation for Statistical Computing, Vienna, Austria), and the data pretreatment procedures include nonlinear retention time alignment, peak discrimination, filtering, alignment, and matching. All detected peaks were tabulated with tR-m/z pairs and outputted for statistical analyses. In order to screen the significant compounds that were responsible for the difference between model and model + EDA, metabolomics strategies were subsequently used to dispose the data. Principal component analysis (PCA), orthogonal partial least-squares discriminant analysis (OPLS-DA), volcano Plot and heatmap developed by Metaboanalyst (https://www.metaboanalyst.ca/) were adopted to do the preliminary screening. PCA is a multivariate technique which can select the typical variables from a data table by several linear transformations and OPLS-DA is a supervised machine learning model. The online database including HMDB (http://www.hmdb.ca/), METLIN (http://metlin.scripps.edu/), and MassBank

(http://www.massbank.jp/) were performed to identify the potential metabolites by matching with the message of ion fragments.

Targeted analysis for taurine by HPLC-QQQ-MS/MS

Targeted analysis was performed on a triple quadrupole tandem high performance liquid chromatography-mass spectrometry (HPLC-QQQ-MS/MS) system (Agilent, 6465) with caffeic acid as the internal standard. Chromatographic separation was performed on a TSK-GEL Amide-80 column (150 × 2.0 mm i.d., 5 μm) with a gradient elution program: 0 - 1 min, 75 - 75% B; 1 - 2 min, 75 - 60% B; 2 - 3min, 60 - 60% B; 3 - 5 min, 60 - 50% B. The mobile phase system consists of deionized water containing 0.1 % formic acid (A) and acetonitrile containing 0.1 % formic acid (B) at a flow rate of 0.2 mL/min. Multiple reaction monitoring transitions in negative mode were performed at m/z124→79.9 for the target analyte taurine, and m/z 179→135 for internal standard compound. MS parameters for the LC-MS/MS system including fragment and voltage collision energy of taurine and internal standard were 110 V, 21 V and 90 V, 17 V, respectively.

Western blot analysis

The RIPA buffer supplemented with protease inhibitor cocktail was adopted for lysing ischemic penumbra of the brain tissues, and obtained samples were used for western blotting as described previously [13]. Protein concentration of tissues were determined by bicinchoninic acid (BCA) protein assay kit (Bi yuntian Biotech. Co., Ltd., China) after centrifuging (12,000 rpm, 10 min, 4℃). The supernatant was diluted by loading buffer to 1 μg/μL followed by heating at 100℃ for 5 min. Equal protein amounts of different groups were electrophoresed on SDS-PAGE gels and transferred to a polyvinylidene fluoride (PVDF) membrane. Then, the obtained PVDF membrane were blocked with 5 % BSA solution for 2 h and incubated with specific primary antibodies overnight at 4℃followed by suitable secondary antibodies at room temperature for 2 h. Protein signals were detected with ECL plus system and imaged by the Gel Imaging System (BioRad, Hercules, CA, USA). The protein levels were calculated by protein signals to correlative GAPDH or β-actin.

Immunofluorescence staining

After perfusion with PBS and 4% paraformaldehyde, brain tissues were picked up and put into 4% paraformaldehyde. After 24 h, brain tissues were dehydrated with 40% sucrose for 5 days, embedded in OTC and frozen at −80℃. Sectioned brain tissues into slices of 10 μm thickness with a cryotome (Leica, Mannheim, Germany). Brain sections were fixed in 4% paraformaldehyde, permeabilized with 0.3% Triton X-100 in PBS, blocked with 5% bovine serum albumin, and incubated with specific primary antibodies overnight at 4℃. Next day, tissue sections were incubated with appropriate fluorescence-conjugated secondary antibodies at room temperature, and cell nucleus was stained with DAPI. The immunofluorescence TUNEL assay was performed according to the instructions of the manufacturer. Fluorescent images were observed by the confocal laser scanning microscopy (CLSM, LSM700, Zeiss, Germany).

Statistical analysis

Student's t test and one-way analysis of variance (ANOVA) followed by Dunnett's post hoc test operating on the Graph Pad Prism 8.0 (Graph Pad Software, La Jolla, CA, USA) were used for analyzing two group comparisons and multiple comparisons, respectively. Differences were considered significant at $P < 0.05$.

Results

EDA effectively ameliorated brain ischemia reperfusion injury in mice

The results of TTC staining demonstrated the marked infarct area of brain appeared after cerebral I/R ($P < 0.0001$) and could be reduced by EDA ($P = 0.0001$) (Fig. 1A-B). H&E staining of brain sections showed that cerebral I/R induced cell loss and numerous vacuolated spaces, whereas EDA ameliorated such histopathological damage, as shown in Fig. 1C. Additionally, the neurobehavioral deficits could be improved by EDA administration compared with model group (*vs.* Sham $P < 0.0001$ and *vs.* Model $P = 0.0027$) (Fig. 1D). The electron microscope was applied for observing the morphology of endothelium, the key element of blood-brain barrier. Obviously, the endothelial cells were destroyed after cerebral I/R and improved by EDA (Fig. 1E). Besides, the activity of LDH in serum was increased in MCAO/R mice ($P < 0.0001$) and could be significantly inhibited by EDA ($P = 0.0004$) (Fig. 1F). Taken together, EDA effectively alleviated the brain injury and inflammation in MCAO/R mice.

Multivariate statistical analysis of urine and serum samples

Analytical stability was validated by contrasting the difference in retention time of the QC samples. The overlapped total ions chromatograms of QC samples showed that retention time deviation was acceptable (Supplementary Fig. 1A-D). Three ions were randomly chosen from QC samples including serum-positive, serum-negative, urine-positive and urine-negative to evaluate the system reproducibility in the metabolomics raw data acquisition throughout the whole experiment. The relative standard deviations (RSD) of the retention times and corresponding peak areas of the 3 selected ions in the QC samples were 0.59–2.54% and 1.14% – 3.78%, as shown in Table 1. The results proved that the repeatability and stability of the HPLC-Q-TOF/MS system were reliable.

Table 1
The relative standard deviation (RSD%) of retention time and peak area in QC samples.

Sample	Model	m/z	Retention time (RSD%)	Peak area (RSD%)
Serum	Positive	203.0541	1.34	2.01
		274.2751	0.95	1.93
		675.6783	1.12	3.56
	Negative	215.0316	1.27	3.78
		809.2477	2.08	2.69
		279.2312	2.54	2.17
Urine	Positive	174.1122	1.83	2.98
		114.0654	0.81	1.74
		263.1456	1.96	3.14
	Negative	172.9869	1.53	1.14
		208.0667	0.59	1.22
		195.0460	1.21	1.65

PCA was applied to perform unsupervised data analysis on Sham, MCAO/R, and EDA groups, and these groups could be easily distinguished from each other (Fig. 2A - D). The phenomenon of EDA group closing to the sham group compared with MCAO/R group showed the improvement of EDA on brain injury. To screen the influential compounds that caused the difference between EDA and model group, OPLS-DA was applied to classify the different samples and select the differential compounds from obtained data. Supplementary Fig. 2A - D suggested that the metabolic profiles in EDA group were significantly different from MCAO/R group in both urine and serum samples, and the ions of variable importance parameters (VIP > 1) were obtained. S-plot was applied to show those changed ions which significantly contributed to the classification between EDA and MCAO/R group (Supplementary Fig. 2E - H). Depending on VIP > 1 and p-value ($p < 0.05$) acquired through two-tailed Student's t-test and showed in volcano plot (Supplementary Fig. 3A - D), the variables can be selected for further screening. According to the above screening procedures, the ions were selected and the metabolites were identified, which were considered as potential biomarkers listed in Table S1-2. The hierarchical clustering heatmap exhibited the change of metabolites more intuitively (Fig. 3A - B). The heatmap showed that EDA and MCAO/R could be grouped into two parts according to the identified metabolites. The above data exposed that numerous metabolites changed by EDA. Among these metabolites, taurine showed the greatest change.

Enrichment analysis of metabolic pathway and regulatory enzymes changed by EDA

In order to comprehensively observe the changes in metabolic pathways, Metaboanalyst 4.0 (https://www.metaboanalyst.ca/) was applied for pathway and biological function enrichment by introducing all significant metabolites of serum and urine. The perturbed pathways including valine, leucine and isoleucine biosynthesis, phenylalanine metabolism, taurine and hypotaurine metabolism were screened out (Fig. 4A - B). And the correlations between biological functions was also showed in Fig. 4C. The results suggested that EDA could improve many pathways under MCAO/R. Moreover, the related regulatory enzymes interaction network built up with STRING (https://string-db.org/) was exhibited in the Supplementary Fig. 4A. And the GO enrichment analysis of related regulatory enzymes performed by Metascape (https://www.metascape.org/) showed that cellular amino acid metabolic process, monocarboxylic acid metabolic process, metabolism of lipids and so on were regulated by EDA (Fig. 4D), and the relations of them were exhibited in Supplementary Fig. 4B. According to the results described above, a schematic diagram of the changed metabolic pathways in serum and urine was exhibited in Fig. 5.

Semiquantitative analysis of taurine and validation of CSAD expression in pre- and post-treatment by EDA

Identification of taurine was characterized by MS profile and confirmed with a standard compound, as shown in Supplementary Fig. 5. Analyses of all samples showed that taurine decreased in MCAO/R mice compared with sham groups ($P < 0.0001$) and could be improved by EDA ($P < 0.0001$) (Fig. 6A). To explore the possible reasons for the change of taurine, the level of CSAD, which is the predominant enzyme regulates taurine biosynthesis in brain was determined. The expression of CSAD in the brain decreased in MCAO/R mice ($P < 0.0017$) and dramatically increased in mice with treatment EDA ($P < 0.0035$) (Fig. 6B). The results of immunofluorescent staining proved that the same tendency of CSAD expression in brain ECs (*vs.* Sham $P = 0.0011$ and *vs.* Model $P = 0.0049$) (Fig. 6C - D). These results demonstrate that the level of taurine was improved by EDA through inhibiting CSAD expression.

EDA alleviates MCAO/R induced brain ECs apoptosis *in vivo*

As shown in Fig. 7A - B, TUNEL assays of brain sections counterstained with CD31 to mark endothelium proved that TUNEL-positive brain ECs increased significantly in the MCAO/R mice ($P = 0.0003$), while the number of TUNEL-positive brain ECs was decreased after treatment with EDA ($P = 0.0015$). The levels of apoptosis related proteins were measured with western blot. The results showed that EDA significantly inhibited the expression of Bax and cleaved caspase-3 (*vs.* Sham $P = 0.0051$ and *vs.* Model $P = 0.0153$), and up-regulated the expression of Bcl-2 comparing with the MCAO/R group (*vs.* Sham $P = 0.0001$ and *vs.* Model $P = 0.0004$) (Fig. 7C - D). These results suggested that EDA had a protective effect on MCAO/R-induced brain ECs apoptosis.

Discussion

In this study, through analysis of high-through metabolomics data and multi-step validations, we attempted to find the untapped therapeutic targets of EDA, a first-line drug for the clinical treatment of

stroke, toward elucidating the therapeutic mechanisms. Initially, we verified that EDA could significantly decrease cerebral infarction, inflammatory infiltration, neurological deficits, endothelium injury and apoptosis in MCAO/R mice. The above investigations showed EDA could effectively alleviate the cerebral ischemia-reperfusion injury in MCAO/R mice, thereby providing reliable samples for subsequent metabolomic analysis.

The results of metabolomic analyses presented the metabolic signature of EDA improvement of cerebral I/R injury offering insights into the therapeutic mechanisms. Comparing EDA and MCAO/R groups, 51 and 56 differential metabolites were identified in serum and urine, respectively. The differential metabolites were mainly lipids, fatty acids in serum and were mainly amino acids in urine. Notably, oleic acid, linoleic acid, triacylglycerol (TG), palmitic acid, prostaglandin I2, urea and leucine were reduced by EDA, while sphingosine-1-phosphate, taurine, valine, glutamine and creatine were improved by EDA, especially taurine and valine. Increased level of oleic acid leads to mitochondrial-derived reactive oxygen species production resulting in endothelial dysfunction and blood brain barrier disruption [14, 15]. Linoleic acid associated with cardiovascular and cerebrovascular diseases significantly activates proinflammatory signaling in ECs, such as PI3K/Akt and ERK1/2, thus causing vessel inflammation, endothelial dysfunction and death [16–19]. Adults with high triacylglycerol have increased risks of incident CHD and stroke, while lowering triglyceride levels of serum improve endothelial function, leading to a decrease in cardiovascular diseases [20–22]. Similarly, elevated palmitic acid level is related to the development of inflammation and endothelial dysfunction [23]. Palmitic acid also induces energy metabolism disorders and apoptosis via activation of the apoptotic mitochondrial pathway [24, 25]. Additionally, excess prostaglandin I2, urea and leucine could similarly result in vascular endothelial injury, and even lead to barrier disruption [26–30]. Vessel inflammation, endothelial dysfunction and death were the main factors causing cardiovascular and cerebrovascular diseases including stroke. The levels of metabolites damaging ECs mentioned above were reduced by EDA, thus improving I/R injury. Sphingosine-1-phosphate, a bioactive intermediate of sphingolipid metabolism, serves important physiological functions, such as proliferation, differentiation, survival, and migration and is a key regulator of lymphocyte trafficking, endothelial barrier function, and vascular tone [31]. Taurine, a sulfur-containing amino acid and known as semi-essential in mammals presents in several organs including brain and demonstrates extensive physiological activities such as anti-inflammation and anti-oxidative stress, as well as regulation of energy metabolism, gene expression, osmosis and quality control of protein. Thus, taurine protects against injuries and toxicities of the nervous system and has potential ameliorating effects against neurological disorder events such as neurodegenerative diseases, stroke, and diabetic neuropathy [32]. Valine, one of the eight essential amino acids and sugarproducing amino acids for human body, could promote the normal growth of the body, regulate protein and energy metabolism and neurological functions [33]. Glutamine metabolism is important for ECs in health and disease conditions, especially in cardiovascular diseases. Glutamine possesses potent antioxidant and anti-inflammatory effects in the circulation, but also drives key processes in vascular cells, including proliferation, migration, apoptosis, senescence, and extracellular matrix deposition by serving as a substrate for synthesis of DNA, ATP, proteins, and lipids [34, 35]. Creatine exhibits ergogenic effects under

a number of conditions including neurodegenerative diseases by maintaining cellular ATP stores. Moreover, creatine could improve ischemic stroke and other cerebrovascular diseases due to antioxidant activity, neurotransmitter-like behavior, prevention of opening of mitochondrial permeability pore [36]. The metabolites described above could replicate some of previous research findings about treatment of stroke. In this study, the level of oleic acid and palmitic acid decreased after treating with EDA, which appears to be in line with the treatment of gross saponins of *Tribulus terrestris* fruit [9]. Similarly, the decrease of phenylalanine was in accord with previous report [8]. However, marked increase of taurine did not happen in these studies.

Subsequently, the pathways mediated by EDA were enriched with the differential metabolites. The results highlighted amino acid metabolisms, fatty acid metabolisms and lipid metabolisms, such as valine, leucine and isoleucine biosynthesis, biosynthesis of unsaturated fatty acids, sphingolipid metabolism as well as taurine and hypotaurine metabolism pathways. The enrichment results of pathways involved regulatory enzymes were similar. As described above, valine, leucine and isoleucine metabolism and most fatty acid metabolisms were directly associated with endothelial dysfunction through increasing reactive oxygen species generation and inflammation, and the change of these pathways as well as taurine and hypotaurine metabolism were the important pathological factors in stroke [14, 16, 30]. Therefore, we speculated that EDA inhibits apoptosis, improves endothelial dysfunction and blood brain barrier function by interfering with these metabolic pathways, resulting in protecting brain impairment induced by ischemia-reperfusion.

ECs is the key part of blood-brain barrier which maintains the normal nerve function and metabolism activity of brain tissue. The death of ECs occurs at primary stage of stroke which play a vital role in the early impairment of neurological functions and may interfere with later recovery [37]. Thus, EC is the potential target mechanism for the treatment of stroke. Interestingly, taurine, one of the mainly increased metabolites, has been reported to have a protective effect on the brain in stroke by down-regulating PARP, NF-κB and activating GABAA, glycine receptors as well as attenuating cell death [38, 39]. EDA may inhibit the death of ECs by increasing the level of taurine. Hence, taurine was selected for the follow-up validation to explore the potential targets of EDA. By suppressing activation of Bax, Bcl-2, cleaved caspase-3 and consequent inhibition of apoptosis, taurine increased by EDA ameliorated cerebral microvascular endothelial dysfunction, thereby alleviated brain injury induced by I/R. Thus, the key regulatory enzymes may be the potential targets of EDA for cerebral protection. CSAD is the key regulatory enzyme of taurine biosynthesis and expresses in brain, while its biofunction in MCAO/R hasn't been clarified yet [40]. The expression of CSAD significantly decreased in MCAO/R mice while increased in mice treatment with EDA. Meanwhile, the ECs apoptosis was inhibited along with expression of CSAD increasing. In summary, given its critical role in inhibiting ECs apoptosis, CSAD has the potential to be developed as a therapeutic target to treat stroke.

Our current study still has several limitations. EDA treats stroke with many complex mechanisms. Numerous differential metabolites and pathways were found to be associated with therapeutic stroke of EDA. Thus, more differential metabolites need to be further investigated.

In the present study, a functional metabolomics strategy was used to characterize metabolite signatures and their underlying mechanisms associated with therapeutic stroke of EDA. We not only constructed the differential metabolic network map providing clues for investigating mechanisms, but also identified the biological function of taurine in the process of EDA treating stroke. It is interesting to note that taurine and its regulatory enzyme CSAD seem to play a key role in inhibiting ECs apoptosis induced by I/R. Therefore, this study elucidated that EDA improve stroke via influence of metabolite providing a reference for finding new therapeutic mechanisms.

Abbreviations

CSAD Cysteine sulfinic acid decarboxylase

EDA Edaravine

LDH Lactate dehydrogenase

MCAO/R Middle cerebral artery occlusion/reperfusion

TUNEL TdT-mediated dUTP nick-end labeling

H&E Haematoxylin and Eosin

EC Endothelial cell

I/R Ischemia/reperfusion

Declarations

Acknowledgments

Not applicable.

Authors' contributions

HF Ma and JP Kou conceived this project and design the experiments. HF Ma and LJ Su performed most experiments and interpreted the data. DW Zhang and YN Liu collected samples. SS Gong, XW Pan aided in the data analysis. HF Ma wrote the manuscript. JP Kou and F Li revised the manuscript. All authors read and approved the final paper.

Funding

This research was supported by funding from the Jiangsu Province Graduate Practice Innovation Program (NO. SJKY190657), and the 'Double First-Class' University Project (CPU2018GF07).

Availability of data and materials

The datasets generated and/or analysed during the current study are available in the HMDB (https://hmdb.ca/), Metaboanalyst (https://www.metaboanalyst.ca/), String (https://string-db.org/) and Metascape (http://metascape.org/).

Ethics approval and consent to participate

Not applicable.

Consent for publication

Not applicable.

Competing interests

The authors declare that they have no competing interests

References

1. Benjamin EJ, Muntner P, Alonso A, Bittencourt MS, Callaway CW, Carson AP, Chamberlain AM, Chang AR, Cheng S, Das SR, et al. Heart disease and stroke statistics-2019 update: a report from the American heart association. Circulation. 2019; 139(10): e56-e528.
2. Montaner J, Ramiro L, Simats A, Tiedt S, Makris K, Jickling GC, Debette S, Sanchez JC, Bustamante A. Multilevel omics for the discovery of biomarkers and therapeutic targets for stroke. Nature reviews. Neurology. 2020; 16(5): 247-64.
3. Kikuchi K, Tancharoen S, Takeshige N, Yoshitomi M, Morioka M, Murai Y, Tanaka E. The efficacy of edaravone (radicut), a free radical scavenger, for cardiovascular disease. Int J Mol Sci. 2013; 14(7): 13909-30.
4. Zhang N, Komine-Kobayashi M, Tanaka R, Liu M, Mizuno Y, Urabe T. Edaravone reduces early accumulation of oxidative products and sequential inflammatory responses after transient focal ischemia in mice brain. Stroke. 2005; 36(10): 2220-5.
5. Amemiya S, Kamiya T, Nito C, Inaba T, Kato K, Ueda M, Shimazaki K, Katayama Y. Anti-apoptotic and neuroprotective effects of edaravone following transient focal ischemia in rats. Eur J Pharmacol. 2005; 516(2): 125-30.
6. Yung HW, Korolchuk S, Tolkovsky AM, Charnock-Jones DS, Burton GJ. Endoplasmic reticulum stress exacerbates ischemia-reperfusion-induced apoptosis through attenuation of Akt protein synthesis in human choriocarcinoma cells. FASEB J. 2007; 21(3): 872-84.
7. Shah SH, Kraus WE, Newgard CB. Metabolomic profiling for the identification of novel biomarkers and mechanisms related to common cardiovascular diseases: form and function. Circulation. 2012; 126(9): 1110-20.
8. Fu X, Wang J, Liao S, Lv Y, Xu D, Yang M, Kong L. (1)H NMR-based metabolomics reveals refined-Huang-Lian-Jie-Du-Decoction (BBG) as a potential ischemic stroke treatment drug with efficacy and

a favorable therapeutic window. Front Pharmacol. 2019; 10: 337.

9. Wang Y, Zhao H, Liu Y, Guo W, Bao Y, Zhang M, Xu T, Xie S, Liu X, Xu Y. GC-MS-based metabolomics to reveal the protective effect of gross saponins of tribulus terrestris fruit against ischemic stroke in rat. Molecules. 2019; 24(4).
10. Cao G, Jiang N, Hu Y, Zhang Y, Wang G, Yin M, Ma X, Zhou K, Qi J, Yu B, et al. Ruscogenin attenuates cerebral ischemia-induced blood-brain barrier dysfunction by suppressing TXNIP/NLRP3 inflammasome activation and the MAPK pathway. Int J Mol Sci. 2016; 17(9).
11. Wang Q, Luo W, Zheng W, Liu Y, Xu H, Zheng G, Dai Z, Zhang W, Chen Y, Chen J. Iron supplement prevents lead-induced disruption of the blood-brain barrier during rat development. Toxicol Appl Pharmacol. 2007; 219(1): 33-41.
12. Peron G, Sut S, Dal Ben S, Voinovich D, Dall'Acqua S. Untargeted UPLC-MS metabolomics reveals multiple changes of urine composition in healthy adult volunteers after consumption of curcuma longa L. extract. Food Res Int. 2020; 127: 108730.
13. Zhai KF, Zheng JR, Tang YM, Li F, Lv YN, Zhang YY, Gao Z, Qi J, Yu BY, Kou JP. The saponin D39 blocks dissociation of non-muscular myosin heavy chain IIA from TNF receptor 2, suppressing tissue factor expression and venous thrombosis. Br J Pharmacol. 2017; 174(17): 2818-31.
14. Gremmels H, Bevers LM, Fledderus JO, Braam B, van Zonneveld AJ, Verhaar MC, Joles JA. Oleic acid increases mitochondrial reactive oxygen species production and decreases endothelial nitric oxide synthase activity in cultured endothelial cells. Eur J Pharmacol. 2015; 751: 67-72.
15. Han HS, Jang JH, Park JS, Kim HJ, Kim JK. Transient blood brain barrier disruption induced by oleic acid is mediated by nitric oxide. Curr Neurovasc Res. 2013; 10(4): 287-96.
16. Hennig B, Lei W, Arzuaga X, Ghosh DD, Saraswathi V, Toborek M. Linoleic acid induces proinflammatory events in vascular endothelial cells via activation of PI3K/Akt and ERK1/2 signaling. J Nutr Biochem. 2006; 17(11): 766-72.
17. Satoh K. Linoleic acid. A novel mechanism of endothelial cell dysfunction. Circ J. 2013; 77(11): 2702-3.
18. Marchix J, Choque B, Kouba M, Fautrel A, Catheline D, Legrand P. Excessive dietary linoleic acid induces proinflammatory markers in rats. J Nutr Biochem. 2015; 26(12): 1434-41.
19. Bin Q, Rao H, Hu JN, Liu R, Fan YW, Li J, Deng ZY, Zhong X, Du FL. The caspase pathway of linoelaidic acid (9t, 12t-c18:2)-induced apoptosis in human umbilical vein endothelial cells. Lipids. 2013(2); 48: 115-26.
20. Lee JS, Chang PY, Zhang Y, Kizer JR, Best LG, Howard BV. Triglyceride and HDL-C dyslipidemia and risks of coronary heart disease and ischemic stroke by glycemic dysregulation status: the strong heart study. Diabetes care. 2017; 40(4): 529-37.
21. Kajikawa M, Maruhashi T, Matsumoto T, Iwamoto Y, Iwamoto A, Oda N, Kishimoto S, Matsui S, Aibara Y, Hidaka T, et al. Relationship between serum triglyceride levels and endothelial function in a large community-based study. Atherosclerosis. 2016; 249: 70-5.

22. Hirano K-i, Ikeda Y, Zaima N, Sakata Y, Matsumiya G. Triglyceride deposit cardiomyovasculopathy. New England J Med. 2008; 359(22): 2396-8.
23. Yang Q, Han L, Li J, Xu H, Liu X, Wang X, Pan C, Lei C, Chen H, Lan X. Activation of Nrf2 by phloretin attenuates palmitic acid-Induced endothelial cell oxidative stress via AMPK-dependent signaling. J Agric Food Chem. 2019; 67(1): 120-31.
24. Wen SY, Velmurugan BK, Day CH, Shen CY, Chun LC, Tsai YC, Lin YM, Chen RJ, Kuo CH, Huang CY. High density lipoprotein (HDL) reverses palmitic acid induced energy metabolism imbalance by switching CD36 and GLUT4 signaling pathways in cardiomyocyte. J Cell Physiol. 2017; 232(11): 3020-9.
25. Adrian L, Lenski M, Tödter K, Heeren J, Böhm M, Laufs U. AMPK prevents palmitic acid-induced apoptosis and lipid accumulation in cardiomyocytes. Lipids. 2017; 52(9): 737-50.
26. De Bock M, Wang N, Decrock E, Bol M, Gadicherla AK, Culot M, Cecchelli R, Bultynck G, Leybaert L. Endothelial calcium dynamics, connexin channels and blood-brain barrier function. Prog Neurobiol. 2013; 108: 1-20.
27. d'Apolito M, Colia AL, Manca E, Pettoello-Mantovani M, Sacco M, Maffione AB, Brownlee M, Giardino I. Urea memory: transient cell exposure to urea causes persistent mitochondrial ROS production and endothelial dysfunction. Toxins. 2018; 10(10).
28. Lau WL, Vaziri ND. Urea, a true uremic toxin: the empire strikes back. Clin Sci (Lond). 2017; 131: 3-12.
29. Dorovini-Zis K, Bowman PD, Betz AL, Goldstein GW. Hyperosmotic urea reversibly opens the tight junctions between brain capillary endothelial cells in cell culture. J Neuropathol Exp Neurol. 1987; 46(2): 130-40.
30. Zhenyukh O, González-Amor M, Rodrigues-Diez RR, Esteban V, Ruiz-Ortega M, Salaices M, Mas S, Briones AM, Egido J. Branched-chain amino acids promote endothelial dysfunction through increased reactive oxygen species generation and inflammation. J Cell Mol Med. 2018; 22(10): 4948-62.
31. Książek M, Chacińska M, Chabowski A, Baranowski M. Sources, metabolism, and regulation of circulating sphingosine-1-phosphate. J Lipid Res. 2015; 56(7): 1271-81.
32. Jakaria M, Azam S, Haque ME, Jo SH, Uddin MS, Kim IS, Choi DK. Taurine and its analogs in neurological disorders: Focus on therapeutic potential and molecular mechanisms. Redox Biol. 2019; 24: 101223.
33. Shimomura Y, Kitaura Y. Physiological and pathological roles of branched-chain amino acids in the regulation of protein and energy metabolism and neurological functions. Pharmacol Res. 2018; 133: 215-7.
34. Rohlenova K, Veys K, Miranda-Santos I, De Bock K, Carmeliet P. Endothelial cell metabolism in health and disease. Trends Cell Biol. 2018; 28(3): 224-36.
35. Durante W. The emerging role of l-glutamine in cardiovascular health and disease. Nutrients. 2019; 11(9).

36. Balestrino M, Sarocchi M, Adriano E, Spallarossa P. Potential of creatine or phosphocreatine supplementation in cerebrovascular disease and in ischemic heart disease. Amino acids. 2016; 48(8): 1955-67.
37. Zille M, Ikhsan M, Jiang Y, Lampe J, Wenzel J, Schwaninger M. The impact of endothelial cell death in the brain and its role after stroke: A systematic review. Cell stress. 2019; 3(11): 330-47.
38. Sun M, Zhao Y, Gu Y, Xu C. Anti-inflammatory mechanism of taurine against ischemic stroke is related to down-regulation of PARP and NF-κB. Amino acids. 2012; 42(5): 1735-47.
39. Wang GH, Jiang ZL, Fan XJ, Zhang L, Li X, Ke KF. Neuroprotective effect of taurine against focal cerebral ischemia in rats possibly mediated by activation of both GABAA and glycine receptors. Neuropharmacology. 2007; 52(5): 1199-209.
40. Park E, Park SY, Dobkin C, Schuller-Levis G. Development of a novel cysteine sulfinic Acid decarboxylase knockout mouse: dietary taurine reduces neonatal mortality. J Amino acids. 2014; 2014: 346809.

Figures

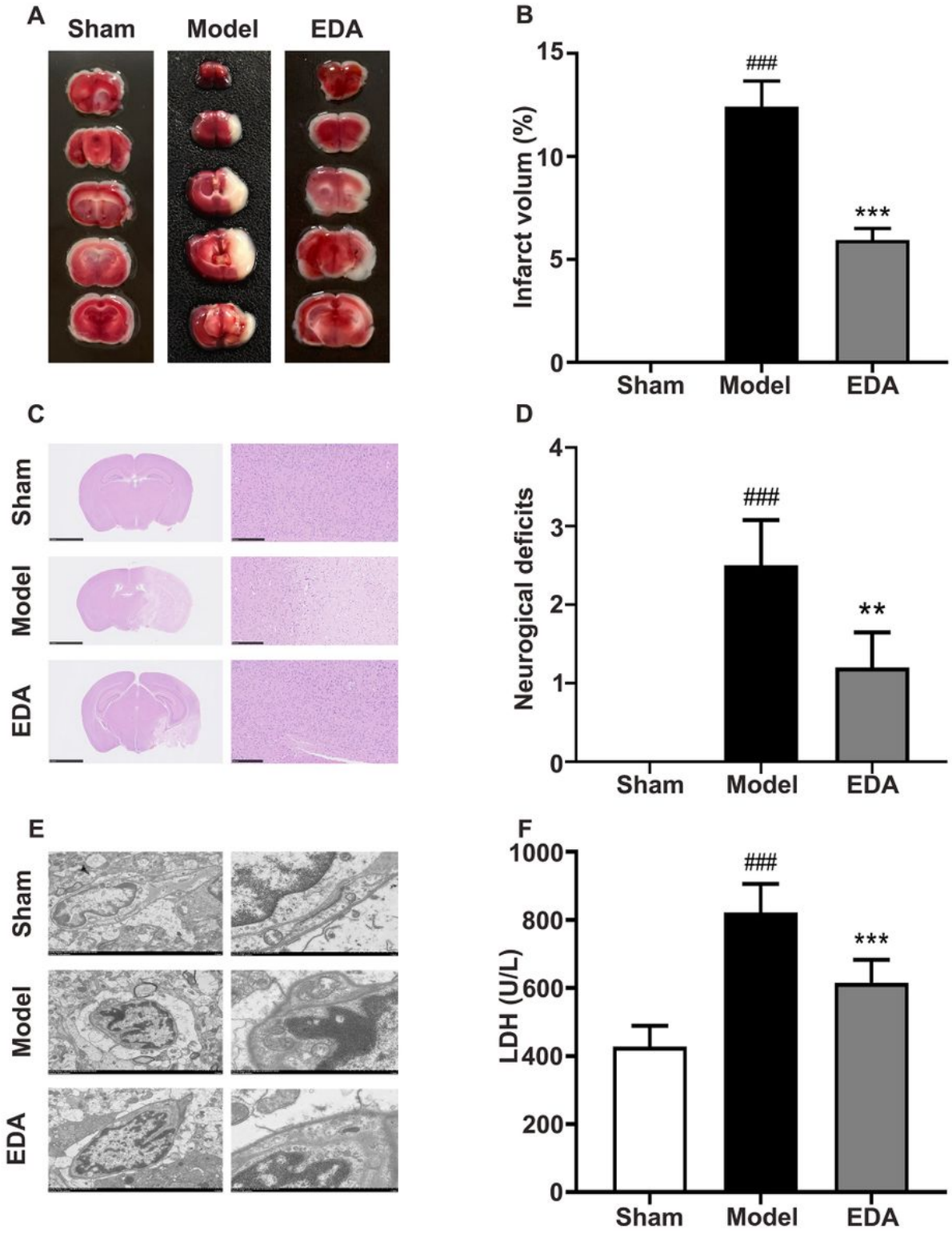

Figure 1

EDA protects against cerebral I/R injury and endothelial injury. Mice were subjected to 1 h of ischemia, followed by 24 h of reperfusion. EDA (3 mg/kg) was administered intraperitoneally after ischemia. (A) Representative TTC-stained brain sections. (B) Quantitative analysis of infarct volume. (C) stained H&E sections of mice brains. (D) Neurological deficit scores in different groups. (E) The structure and morphology of cerebral microvascular endothelial cells in different groups were examined by electron

microscopy. (F) LDH activity. All data are presented as the means ± SD, n = 6. #P < 0.05, ##P < 0.01, ###P < 0.001, vs. Sham group, *P<0.05, **P<0.01, ***P<0.001, vs. MCAO/R group.

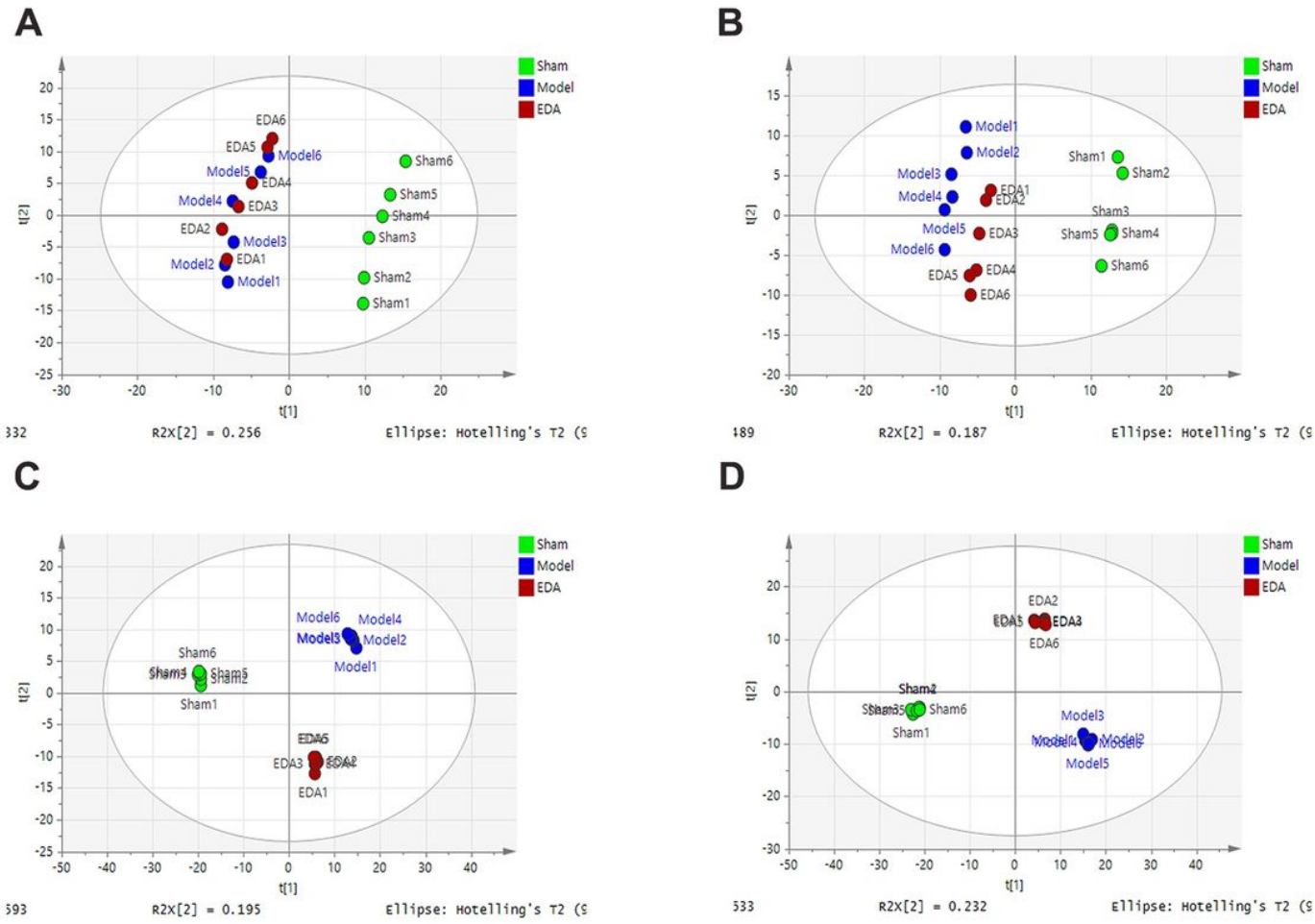

Figure 2

PCA scores plot of sham, model and EDA group based on HPLC-Q-TOF/MS system for serum (A, B) and urine (C, D) analysis.

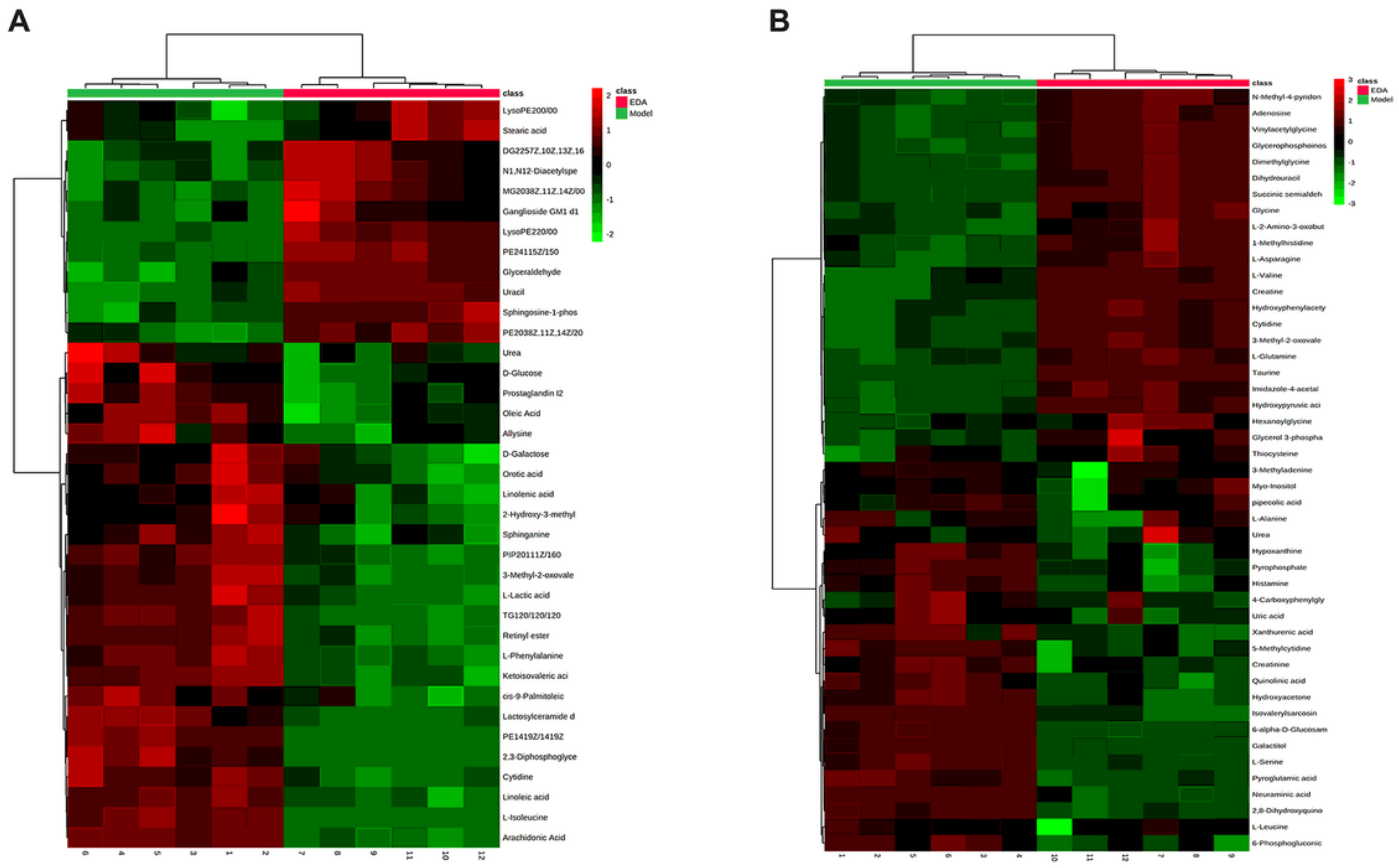

Figure 3

Heat map of the differential endogenous metabolites between the model and EDA group in serum (A) and urine (B). Red represented the metabolites in high abundance, green represented the metabolites in low abundance.

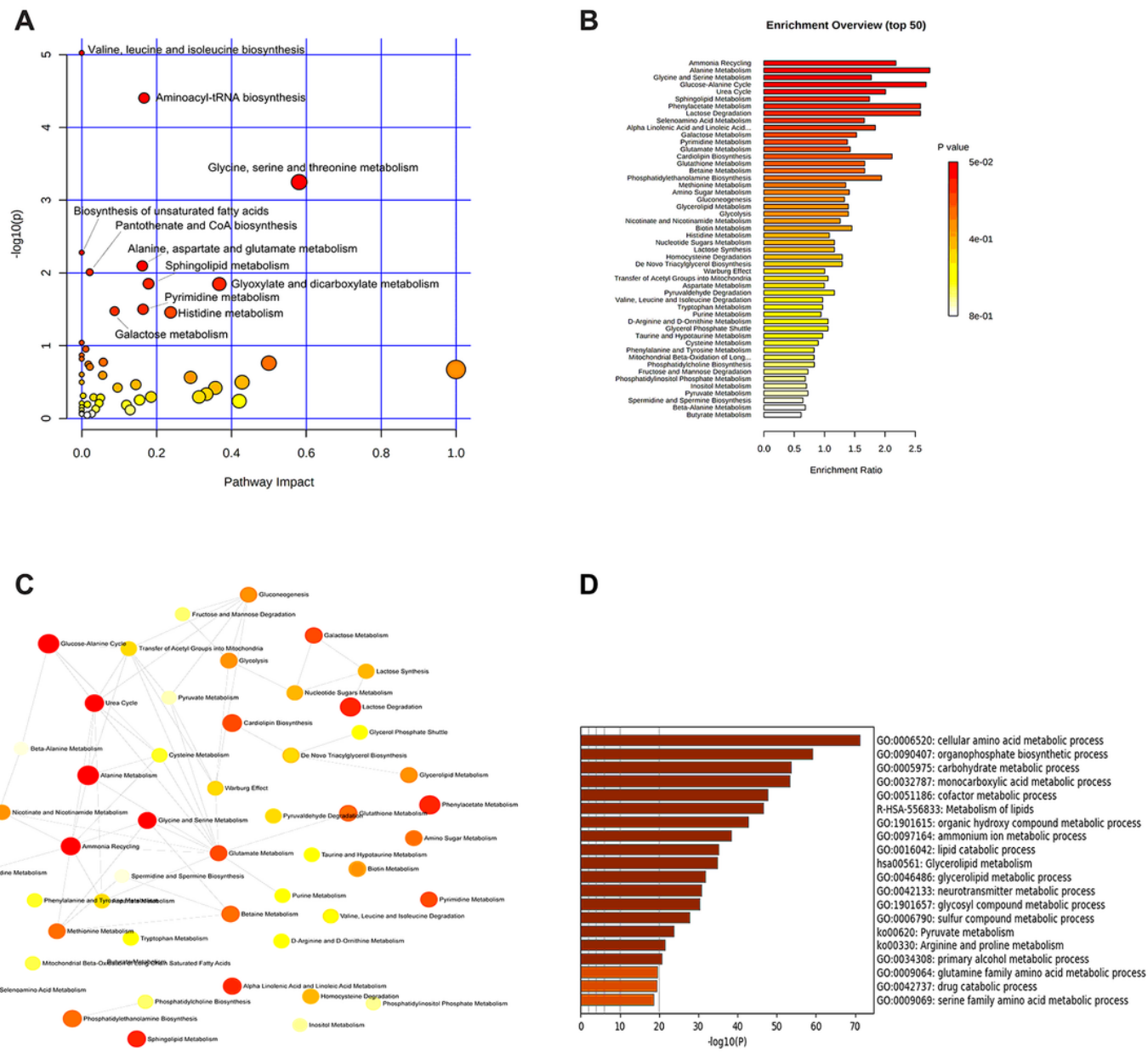

Figure 4

Enrichment analysis of metabolic pathway and related regulatory enzymes. (A) The bubble plots of altered metabolic pathways. (B) Overview of biological function related to the differential endogenous metabolites. (C) The network map of pathways. (D) Regulatory enzyme GO enrichment analysis results.

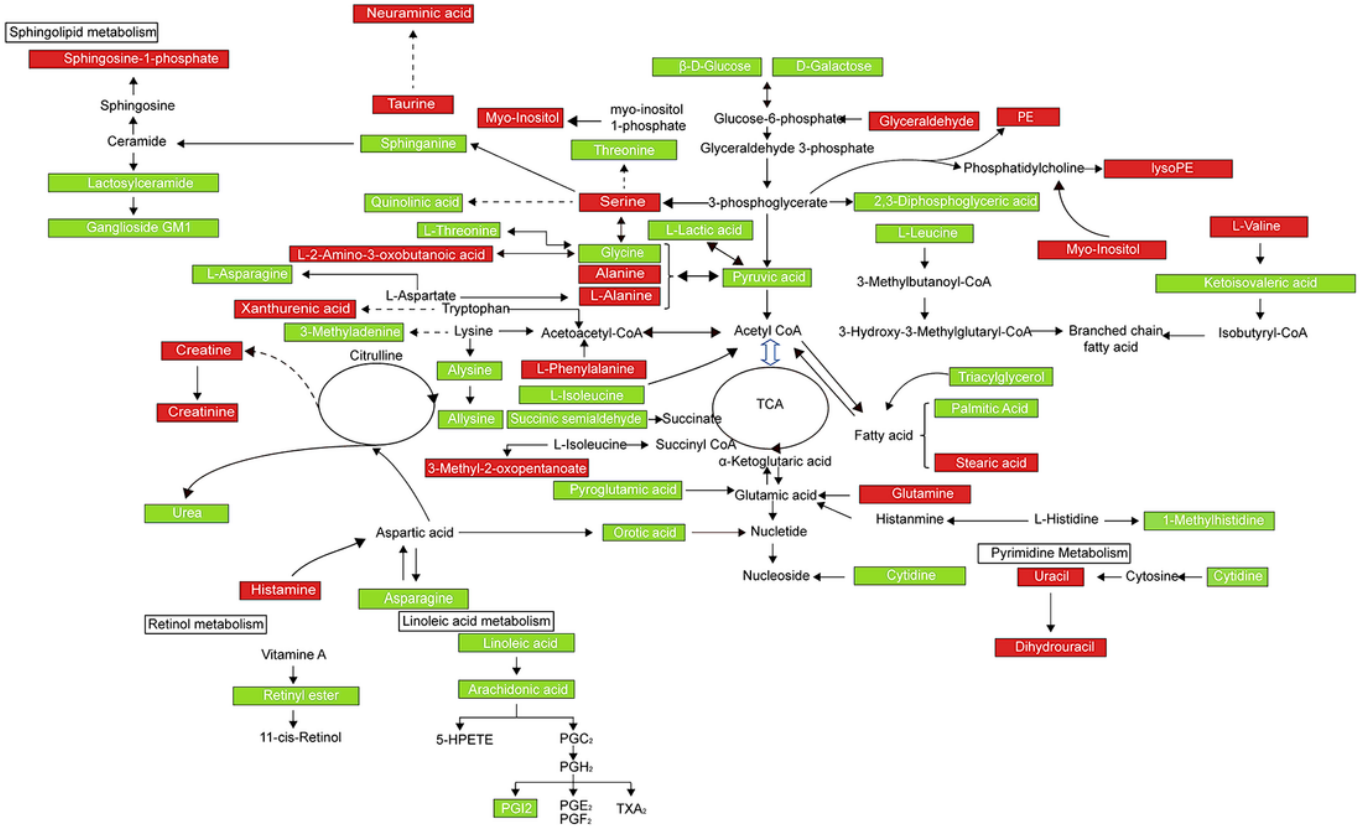

Figure 5

Metabolic network of the significantly changed endogenous metabolites in both serum and urine. Compared with the model group, elevated metabolites in the EDA group were represented by red, and the reduced metabolites were represented by green.

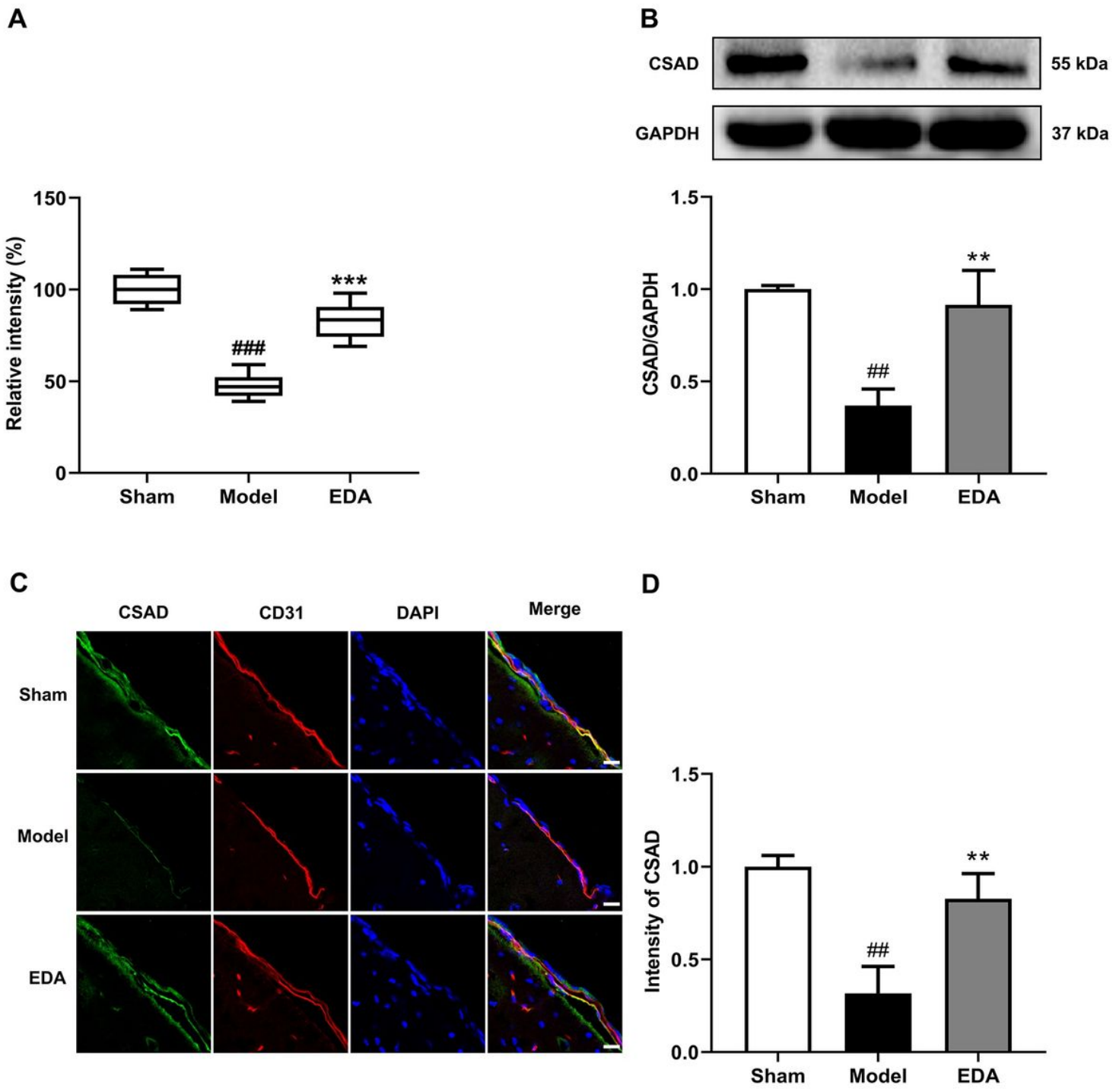

Figure 6

Effect of EDA on taurine and CSAD in MCAO/R mice. (A) The level of taurine in the different groups. (B) Representative Western blots and quantitative analyses of CSAD expression. (C) Immunofluorescence staining for CSAD (green) and CD31 (red) were performed on frozen brain sections, and the nuclei were counterstained with DAPI (blue). Scale bar =20 μm. (D) Quantitative analyses of CSAD expression in endothelial cells. All data are presented as the means ± SD, n = 6. #P < 0.05, ##P < 0.01, ###P < 0.001, vs. Sham group, *P<0.05, **P<0.01, ***P<0.001, vs. MCAO/R group.

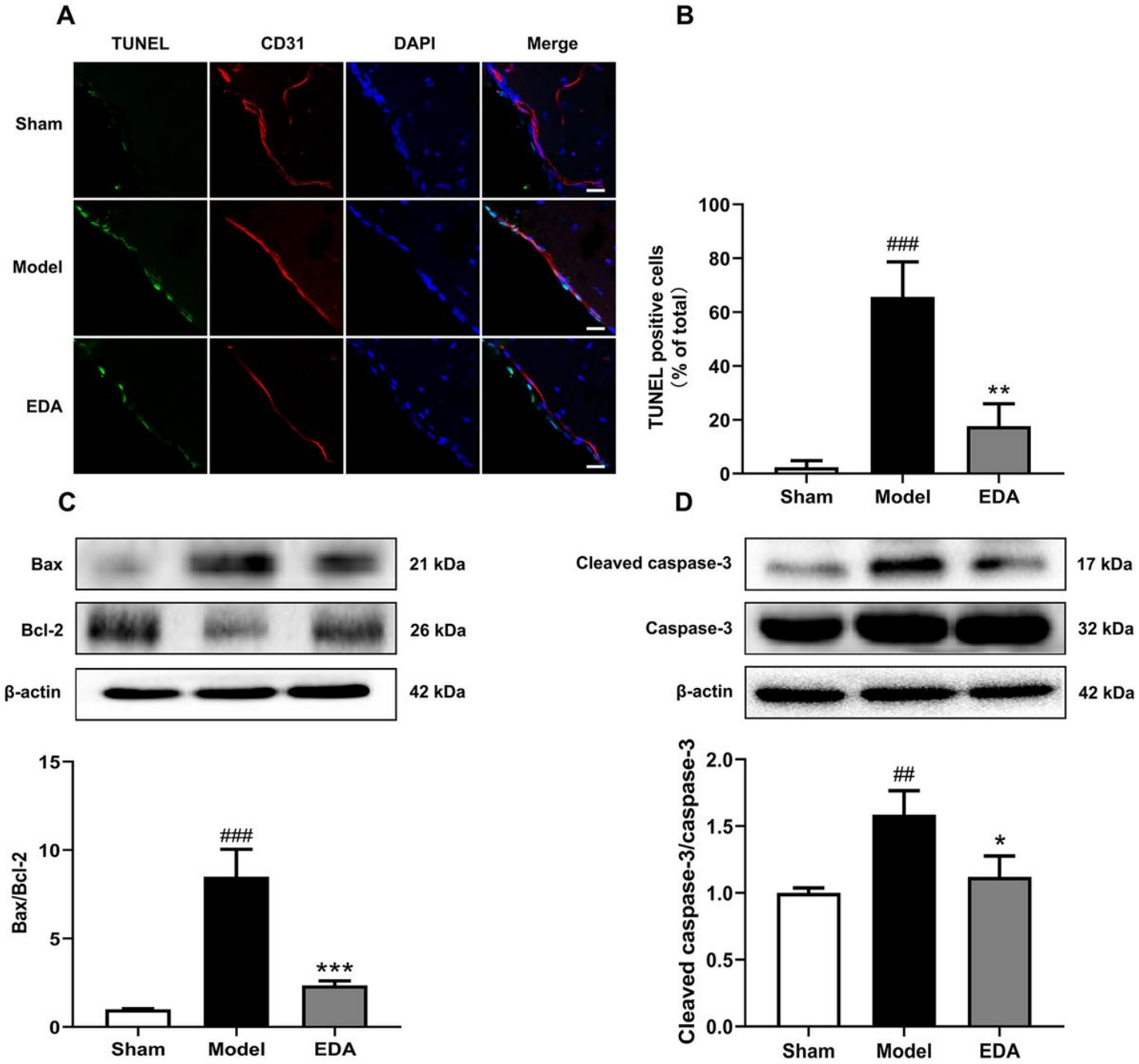

Figure 7

EDA mitigates cerebral endothelial apoptosis stimulated by MCAO/R in mice. (A) Brain frozen sections were stained with TUNEL (green) and CD31 was used as a marker for endothelial cells, the nuclei were stained with DAPI (blue). Scale bar =20 μm. (B) Quantitative analyses of apoptotic cells in endothelial cells. (C) Western blot analysis for the expression of Bax and Bcl-2 in brain tissues. (D) Western blot analysis for the expression of cleaved caspase-3 in brain tissues. All data are presented as the means ± SD, n = 6. #P < 0.05, ##P < 0.01, ###P < 0.001, vs. Sham group, *P<0.05, **P<0.01, ***P<0.001, vs. MCAO/R group.

Supplementary Files

This is a list of supplementary files associated with this preprint. Click to download.

- SupplementaryTable1.docx
- SupplementaryTable2.docx
- Supplementarymaterials1.docx
- Supplementarymaterials2.doc